Journal of Solid State Chemistry **160,** 77–87 (2001)
doi:10.1006/jssc.2001.9194, available online at http://www.idealibrary.com on IDEAL®

Preparation, Properties, and Crystal Structure of the Rare Earth Ruthenium Carbides $R_3Ru_2C_5$ (R = Y, Gd–Er)

Marc W. Pohlkamp, Rolf-Dieter Hoffmann, Gunter Kotzyba, and Wolfgang Jeitschko[1]

Anorganisch-Chemisches Institut, Universität Münster, Wilhelm-Klemm Strasse 8, D-48149 Münster, Germany

Received January 16, 2001; in revised form March 22, 2001; accepted March 26, 2001; published online June 4, 2001

The title compounds were prepared from the elemental components by arc-melting and subsequent annealing. While $Gd_3Ru_2C_5$ and $Tb_3Ru_2C_5$ are present in the as-cast samples, the others are formed during the annealing process. The magnetic properties of the four compounds $R_3Ru_2C_5$ (R = Gd–Ho) were investigated with a SQUID magnetometer. They show very soft ferromagnetism. The highest Curie temperature was observed for the gadolinium compound with $T_C = 84(1)$ K. Electrical conductivity measurements for $Tb_3Ru_2C_5$ indicate metallic behavior. The crystal structure of these isotypic compounds has been determined from single-crystal X-ray data of $Gd_3Ru_2C_5$: $P6_3/m$, $Z = 4$, $a = 1147.0(1)$ pm, $c = 504.7(1)$ pm, $R = 0.052$ for 500 F values and 43 variable parameters. Structure refinements of another crystal of the gadolinium compound with a slightly different composition and of the terbium compound gave similar results. In all three structure refinements a ruthenium position on the hexagonal axis had to be refined with split occupancy. The adjacent lanthanoid positions reflect this disorder. The refinement of the occupancy parameters of the three data sets resulted in the compositions $Gd_3Ru_{1.851(1)}C_{4.86(2)}$, $Gd_3Ru_{1.862(2)}C_{4.97(3)}$, and $Tb_3Ru_{1.776(4)}C_{4.95(1)}$. The structure contains C_2 pairs and isolated carbon atoms. The C–C distances in the three refinements vary between 133(1) and 142(3) pm, close to the typical double-bond distance of 134 pm. The structure contains trigonal polyanionic clusters of the composition Ru_3C_{10}, and in addition there are ruthenium atoms which have no carbon neighbors. Chemical bonding in these compounds is briefly discussed on the basis of the 18- and 8-electron rules. © 2001 Academic Press

INTRODUCTION

A large number of ternary carbides of the rare earth elements with transition metals have been synthesized in recent years. With ruthenium as transition metal component the perovskite ($CaTiO_3$)-type carbides $ScRu_3C$ (1) and $CeRu_3C_{1-x}$ (2, 3) are known for some time. More recently, the isotypic series RRu_3C (R = Dy–Lu) has been reported (4). In these carbides the carbon atoms are isolated from each other and occupy octahedral voids formed by the ruthenium atoms. Carbon pairs were found in the structures of Sc_3RuC_4 (5), $R_{3.67}RuC_6$ (R = La–Nd, Sm, Gd) (6, 7), and $GdRuC_2$ (8). The carbides $R_7Ru_2C_{11}$ (R = Dy–Tm) (9), and $R_{10}Ru_{10}C_{19}$ (R = Y, Gd–Lu) (10) have isolated carbon atoms as well as carbon pairs. Here we report on a new series of carbides $R_3Ru_2C_5$, again with isolated carbon atoms and carbon pairs. A preliminary account about the crystal structure of these compounds has been given at a conference (11).

SAMPLE PREPARATION AND LATTICE CONSTANTS

The samples were prepared by arc-melting of the elemental components. Starting materials were large pieces of the rare earth metals (all with nominal purity > 99.9%). Filings of these were prepared under dry (Na) paraffin oil. The latter was removed by dry hexane. The filings were stored under vacuum and only briefly exposed to air prior to the reactions. The ruthenium was purchased in the form of powder (> 99.9%) and graphite in the form of flakes (> 99.5%). Cold-pressed pellets (~ 0.5 g) of the elemental components were reacted in an arc-melting furnace under an argon atmosphere, which was further purified by repeatedly melting a titanium button prior to the reactions. The sample buttons were melted two or three times and turned around between the melting operations to enhance their homogeneity. Material losses were of the order of 2–3%. The compact samples were wrapped in tantalum foil, sealed in evacuated silica tubes, and annealed for 14 days at 1000°C. They were then quenched in ice water.

The single-crystals of $Gd_3Ru_2C_5$ and $Tb_3Ru_2C_5$ used for the X-ray investigations were obtained by annealing arc-melted samples in a water-cooled silica tube in a high-frequency furnace slightly below the melting temperature for 2 h, followed by annealing for 14 days at 1000°C. The

Additional crystallographic data may be obtained from the Fachinformationsentrum Karlsruhe, D-76344 Eggenstein–Leopoldshafen, Germany, by quoting the registry numbers CSD-411870 ($Gd_3Ru_2C_5$-I) and CSD-411869 ($Tb_3Ru_2C_5$).

[1]To whom correspondence should be addressed.

0022-4596/01 $35.00

TABLE 1
Lattice Constants of Hexagonal Carbides with $Gd_3Ru_2C_5$-Type Structure

Compound	Sample composition (at.%)	Annealing temp. (°C)	a (pm)	c (pm)	c/a	V (nm^3)
$Y_3Ru_2C_5$	35:20:45	1000	1138.4(3)	498.9(1)	0.4382	0.5599
$Gd_3Ru_2C_5$	35:20:45	900	1148.5(3)	506.5(1)	0.4410	0.5786
$Gd_3Ru_2C_5$	37:13:50	1000	1147.3(4)	502.4(2)	0.4379	0.5727
$Gd_3Ru_2C_5$	40:10:50	1000	1135.7(2)	498.0(1)	0.4385	0.5563
$Tb_3Ru_2C_5$	35:20:45	900	1143.4(5)	503.4(1)	0.4403	0.5699
$Tb_3Ru_2C_5$	39:11:50	1000	1131.4(2)	494.7(1)	0.4372	0.5484
$Dy_3Ru_2C_5$	35:20:45	1000	1139.6(3)	500.7(1)	0.4394	0.5632
$Ho_3Ru_2C_5$	35:20:45	1000	1136.5(2)	498.4(1)	0.4385	0.5575
$Er_3Ru_2C_5$	35:20:45	1000	1133.8(4)	495.3(2)	0.4368	0.5514

latter annealing was intended to obtain well ordered samples, however, as revealed by the X-ray investigations without success. The two single-crystals of $Gd_3Ru_2C_5$ were selected from two samples, both with the same nominal composition of Gd:Ru:C = 35:20:45. The single-crystal of $Tb_3Ru_2C_5$ was isolated from a sample with the composition Tb:Ru:C = 39:11:50. Energy-dispersive X-ray analyses in a scanning microscope did not reveal any impurity elements heavier than sodium within the detection limits of *ca* 2 at.%.

The samples were characterized by their Guinier powder patterns using monochromated Cu$K\alpha_1$ radiation and α-quartz ($a = 491.30$ pm and $c = 540.46$ pm) as an internal standard. All samples contained minor amounts of the Laves phases RRu_2. Indices for the new carbides $R_3Ru_2C_5$ could be assigned on the basis of the hexagonal cell found by the single-crystal investigation of $Gd_3Ru_2C_5$. The identification of the diffraction lines was facilitated by intensity calculations (12) using the positional parameters of the structure determinations. The lattice constants listed in Table 1 were obtained by least-squares fits. For several compounds lattice constants were determined from samples with different overall compositions, resulting in differing lattice constants and cell volumes. The latter are shown in Fig. 1.

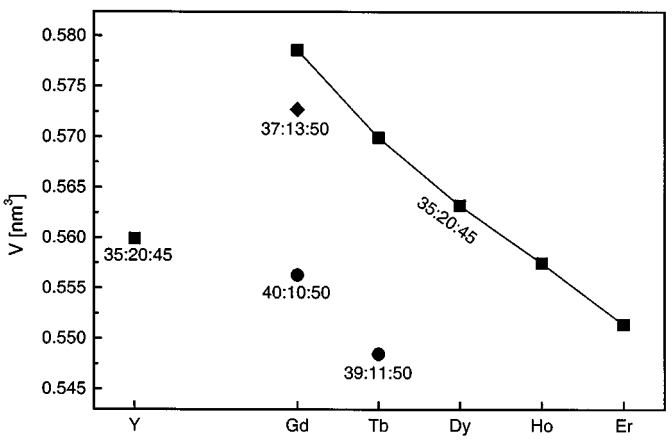

FIG. 1. Cell volumes of the carbides $R_3Ru_2C_5$ with R = Y, Gd–Er. The compounds have homogeneity ranges. Therefore, the lattice constants depend on the compositions of the samples. The overall sample compositions are given in atomic ratios R:Ru:C.

PROPERTIES

The compact samples have a dark gray color with some luster, like elemental silicon. The powders are black and stable on air for long periods of time.

Magnetic Susceptibilities

The magnetic properties of powder samples of the four compounds $R_3Ru_2C_5$ (R = Gd–Ho) were investigated with a superconducting quantum interference device (SQUID) magnetometer (Quantum Design, MPMS) in the temperature range between 2 and 300 K with magnetic flux densities up to 5.5 T. About 30 mg of each sample was put in a thin-walled silica tube (inner diameter 2 mm). The samples were held in place by compression with a cotton plug. In general, the samples were cooled in zero field and the magnetic susceptibilities were recorded continuously on heating. To check for ferromagnetic impurities the samples were investigated at 300 K with various magnetic flux densities. Only the sample of the yttrium compound had a strong field dependence at that temperature, indicating a ferromagnetic impurity. For that reason this sample was not investigated any further. The results for the other samples are shown in Fig. 2.

The reciprocal susceptibilities of the four compounds $R_3Ru_2C_5$ (R = Gd–Ho) show Curie–Weiss behavior (left-hand side of Fig. 2). From the linear portions of the reciprocal susceptibility plots above 150 K, recorded with a magnetic flux density of 3 T, we obtained paramagnetic Curie temperatures (Weiss constants Θ) between 71 ± 3 K for $Gd_3Ru_2C_5$ and 5 ± 3 K for $Ho_3Ru_2C_5$. The corresponding experimentally determined effective magnetic moments,

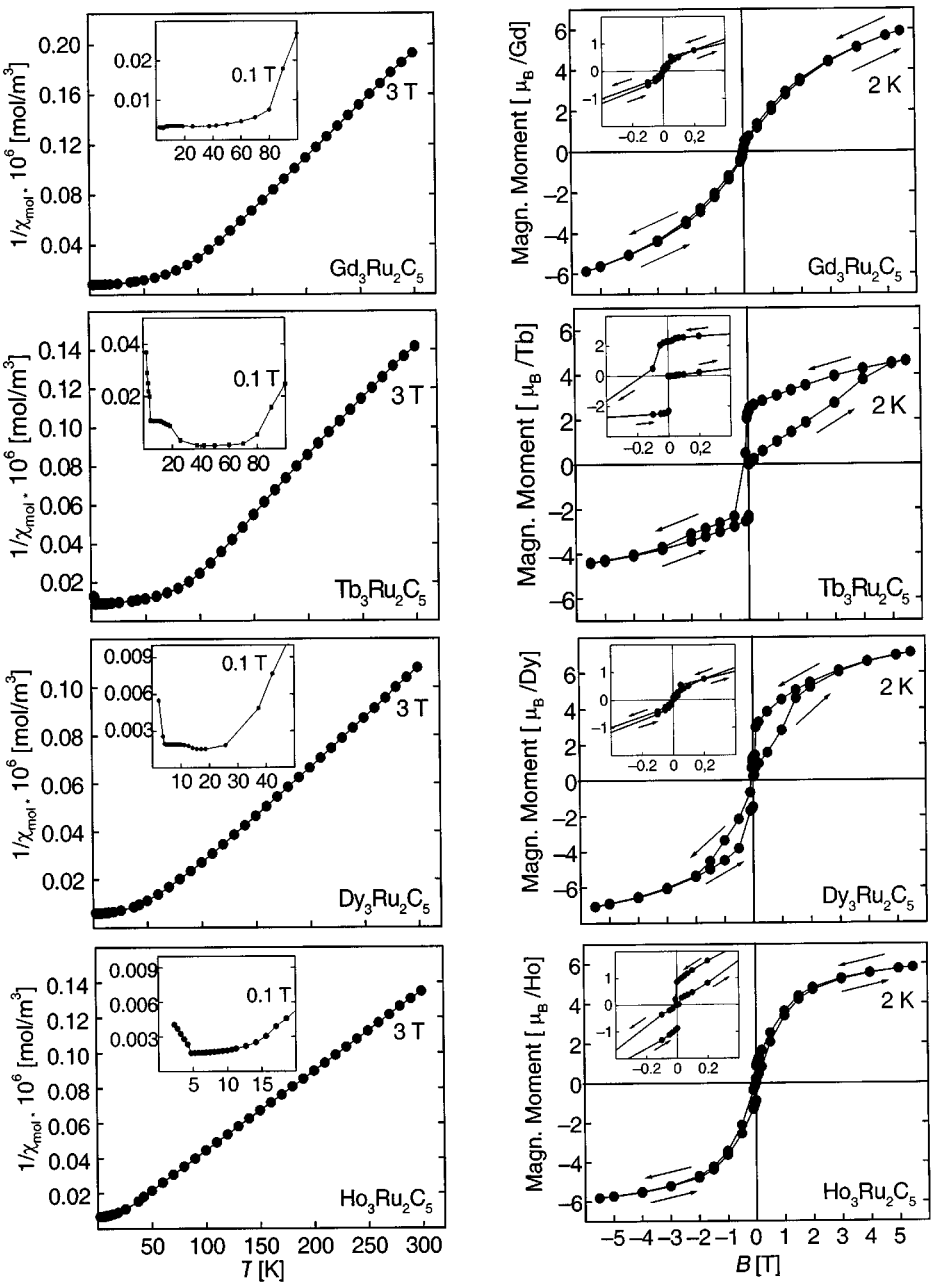

FIG. 2. Reciprocal susceptibilities and magnetization curves of the ferromagnetic carbides $R_3Ru_2C_5$ (R = Gd–Ho). The reciprocal susceptibilities of the main plots were recorded with a magnetic flux density of 3 T, for the insets with 0.1 T. The magnetization curves were all recorded at a temperature of 2 K. The insets show the magnetization behavior at low magnetic flux densities B.

calculated from the relation $\mu_{exp} = 2.83\,[(\chi/3)(T-\Theta)]^{1/2}(4\pi\times10^{-6})^{-1/2}$ are generally in good agreement with the theoretical moments μ_{eff} for the free R^{3+} ions (Table 2). The only exception is the dysprosium compound, where the experimentally determined magnetic moment of $\mu_{exp} = 11.35(3)\,\mu_B$ is slightly higher than the theoretical one of $\mu_{eff} = 10.65\,\mu_B$. This difference might be ascribed to an unknown impurity with a high content of dysprosium.

The positive values of the Weiss constants indicate ferromagnetic order. This was confirmed by the magnetization measurements carried out at 2 K, shown in the right-hand diagrams of Fig. 2. The Curie temperatures T_C vary between 84 ± 1 K for $Gd_3Ru_2C_5$ and 12 ± 1 K for $Ho_3Ru_2C_5$ (Table 2). They were determined by "kink-point" measurements (not shown). For this purpose each sample was cooled in a weak magnetic field (0.002 T) to low

TABLE 2
Magnetic Data of the Ferromagnetic Carbides $R_3Ru_2C_5$ (R = Gd–Ho)[a]

Compound	μ_{exp} (μ_B/R^{3+})	μ_{eff} (μ_B/R^{3+})	Θ (K)	T_C (K)	$\mu_{exp(sm)}$ (μ_B/R^{3+})	$\mu_{calc(sm)}$ (μ_B/R^{3+})
$Gd_3Ru_2C_5$	7.94(5)	7.94	71(3)	84(1)	5.91(3)	7.00
$Tb_3Ru_2C_5$	9.74(5)	9.72	47(5)	78(1)	4.60(3)	9.00
$Dy_3Ru_2C_5$	11.35(3)	10.65	38(3)	22(1)	7.15(3)	10.00
$Ho_3Ru_2C_5$	10.78(5)	10.61	5(3)	12(1)	5.88(3)	10.00

[a] The experimentally determined effective moments, μ_{exp}, obtained from the slopes of the $1/\chi$ vs T plots, are compared with the corresponding theoretical moments, calculated from the relation $\mu_{eff} = g[J(J+1)]^{1/2}$. The highest magnetic moments $\mu_{exp(sm)}$ of the magnetization curves observed at 5.5 T are listed together with the theoretical saturation magnetizations obtained from the equation $\mu_{calc(sm)} = g \cdot J$. The Weiss constants Θ and the Curie temperatures T_C are also given.

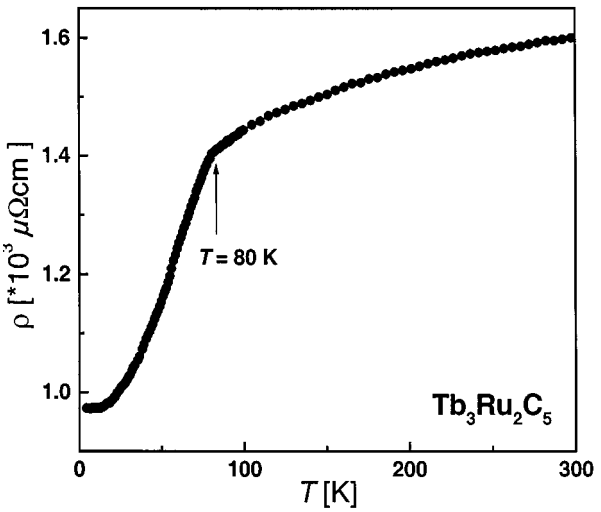

FIG. 3. Electrical resistivity of $Tb_3Ru_2C_5$ as a function of temperature. The discontinuity in the plot at 80 K corresponds to the Curie temperature.

temperatures, and the turning point of the thus obtained magnetic susceptibility curve was determined by calculating its derivative. This turning point was considered as the Curie temperature. The magnetization curves for the four carbides $R_3Ru_2C_5$ (R = Gd–Ho) show only small hysteresis loops, indicating very soft ferromagnetism. For the holmium compound the hysteresis is very small because it was recorded (at 2 K) only 10 K lower than the Curie temperature of $T_C = 12$ K. The hysteresis of $Gd_3Ru_2C_5$ is even smaller, practically not visible, and this apparently has to do with the half-filled f shell of Gd^{3+}. Such exceptional magnetic behavior is frequently observed for gadolinium compounds (13–16). In none of the magnetization curves were we able to reach the saturation magnetization at $\pm$ 5.5 T, the highest magnetic flux density attainable with our SQUID magnetometer. This can be seen from the shapes of the magnetization curves as well as from the values of the experimental "saturation" magnetizations $\mu_{exp(sm)}$, which amount to 84, 51, 72, and 59% of the theoretically attainable saturation magnetizations $\mu_{calc(sm)}$ for the compounds $R_3Ru_2C_5$ with R = Gd, Tb, Dy, and Ho, respectively (Table 2).

Electrical Conductivity

Using $Tb_3Ru_2C_5$ as an example, we have determined the electrical conductivity behavior of these carbides. A poly-

TABLE 3
Crystal Data for $Gd_3Ru_2C_5$ and $Tb_3Ru_2C_5$

Compound	$Gd_3Ru_2C_5$ (I)	$Gd_3Ru_2C_5$ (II)	$Tb_3Ru_2C_5$
Space group	$P6_3/m$	$P6_3/m$	$P6_3/m$
a (pm)	1147.0(1)	1145.0(2)	1130.4(2)
c (pm)	504.7(1)	502.0(1)	494.6(1)
V (nm^3)	0.5750	0.5699	0.5473
Pearson symbol	$hP50$–11.2	$hP50$–10.7	$hP50$-11.1
Formula units/cell (Z)	4	4	4
Composition	$Gd_3Ru_{1.851(1)}C_{4.86(2)}$	$Gd_3Ru_{1.862(2)}C_{4.97(3)}$	$Tb_3Ru_{1.776(4)}C_{4.95(1)}$
Formula mass	717.2	719.6	715.7
Calculated density (g/cm^3)	8.28	8.39	8.69
Crystal dimensions (μm^3)	$5 \times 5 \times 40$	$22 \times 22 \times 66$	$33 \times 33 \times 88$
$\theta/2\theta$ Scans up to 2θ	69.9°	65.9°	63.8°
Range in h, k, l	0–18, $\pm$ 18, 0–8	$\pm$ 17, $\pm$ 17, $\pm$ 7	$\pm$ 16, $\pm$ 16, $-1 < l < 6$
Total No. of reflections	3379	8512	3851
Unique reflections	923	785	645
Internal residual (on F^2)	0.090	0.107	0.137
Reflections with $I_0 > 2\sigma(I_0)$	500	490	420
No. of variables	43	43	43
R (No. of F)	0.052 (500)	0.028 (490)	0.065 (420)
R_w (No. of F^2)	0.070 (923)	0.060 (785)	0.088 (645)
Largest diff. peak/hole (e/Å^3)	3.15/ $-$ 3.56	3.93/ $-$ 4.12	4.18/ $-$ 4.98

crystalline compact fragment (with a diameter of approximately 0.5 mm) of an annealed arc-melted button was investigated with a four-probe technique as described earlier (17–20). Due to the difficulty in estimating the sizes of the contacted areas the absolute values of the resistivities are correct only within a factor of ± 2. The relative resistivities at different temperatures, however, are much more reliable. The electrical resistivity of $Tb_3Ru_2C_5$ increases from 4 K to room temperature (Fig. 3), thus indicating metallic behavior. The discontinuity in the resistivity curve observed at 80 K corresponds to the Curie temperature which had been found at 78 ± 1 K by the magnetic susceptibility measurements.

STRUCTURE DETERMINATION AND REFINEMENTS

The structure determination was carried out at first with a single-crystal of the gadolinium compound (I). The refinement of this structure resulted in some split and disordered positions, and for that reason another crystal (II) of this compound, and in addition a crystal of the terbium compound, were used for structure refinements, all with very similar results.

Single-crystals were isolated from crushed samples prepared by arc-melting and further annealing as described above. They were selected on the basis of Laue and precession diagrams. Intensity data were collected for three single-crystals on a four-circle diffractometer (Enraf Nonius, CAD4) with graphite-monochromated Mo$K\alpha$ radiation and a scintillation counter with a pulse-height discriminator. The scans were along θ with background counts at both ends of each scan. Empirical absorption corrections were made on the basis of psi-scans. Further details of the data collections are summarized in Table 3.

The data sets showed the low hexagonal Laue symmetry $6/m$ and the structures were eventually all refined in the centrosymmetric space group $P6_3/m$ (No. 176). The positions of most metal atoms were obtained from a Patterson synthesis and the other atoms were located by difference Fourier computations. For the final structure refinements a full-matrix least-squares program was used (21) with atomic scattering factors, corrected for anomalous dispersion, as provided by the program. The weighting scheme accounted for the counting statistics, and a parameter correcting for isotropic secondary extinction was optimized as a least-squares variable.

There were some difficulties in the refinements of the atomic positions on the threefold axes. The 4*f* position $\frac{1}{3}, \frac{2}{3}, z$ with $z \sim 0$ has an octahedral environment of $3R2 + 3Ru1$. In view of this coordination it is suited only for carbon atoms (the C4 atoms), and the refinements of the occupancy parameters showed that at most only every other of the face-sharing R_3Ru_3 octahedra contains a carbon atom. The 4*e* position 0, 0, *z* shows a much higher scattering power. It is surrounded by *R* atoms, and the interatomic distances are so short that only ruthenium atoms (Ru2) are suited for this site. The refinement of the occupancy parameters for this site resulted in occupancies close to 1/3 for the two crystals of $Gd_3Ru_2C_5$ and the crystal of $Tb_3Ru_2C_5$ (Table 4). This partial occupancy of the Ru2 site makes it possible to rationalize the split *R*1 positions (*R*1a and *R*1b) which were refined with constrained occupancies. It was possible to refine thermal parameters together with variable occupancies in all cases including the C4 positions.

We have also refined the occupancy values of the other atomic sites, again together with variable displacement parameters, while the scale factor was fixed. The resulting occupancy parameters for the crystal $Gd_3Ru_2C_5$ (I) were as follows: Gd2, 100.9(3); Ru1, 99.2(5); C1, 103(5); C2, 98(5); and

TABLE 4
Atomic Parameters of $Gd_3Ru_2C_5$ and $Tb_3Ru_2C_5$[a]

Atom	$P6_3/m$	Occupancy	x	y	z	U
$Gd_3Ru_{1.851(1)}C_{4.86(2)}$ (I)						
Gd1a	6*h*	0.753(1)	0.2597(1)	0.2599(1)	$\frac{1}{4}$	87(1)
Gd1b	6*h*	0.247(1)	0.2182(2)	0.2200(2)	$\frac{1}{4}$	31(6)
Gd2	6*h*	1	0.5070(1)	0.1233(1)	$\frac{1}{4}$	90(1)
Ru1	6*h*	1	0.2056(1)	0.5028(1)	$\frac{1}{4}$	89(1)
Ru2	4*e*	0.351(1)	0	0	0.0654(2)	94(5)
C1	6*h*	1	0.0686(6)	0.3218(7)	$\frac{1}{4}$	72(3)
C2	6*h*	1	0.2074(9)	0.0188(8)	$\frac{1}{4}$	75(5)
C3	6*h*	1	0.1199(6)	0.6116(7)	$\frac{1}{4}$	67(7)
C4	4*f*	0.36(2)	$\frac{1}{3}$	$\frac{2}{3}$	0.0014(6)	75(4)
$Gd_3Ru_{1.862(2)}C_{4.97(3)}$ (II)						
Gd1a	6*h*	0.738(1)	0.2638(2)	0.2634(2)	$\frac{1}{4}$	83(1)
Gd1b	6*h*	0.262(1)	0.2240(2)	0.2225(2)	$\frac{1}{4}$	91(4)
Gd2	6*h*	1	0.1279(1)	0.5071(1)	$\frac{1}{4}$	45(1)
Ru1	6*h*	1	0.5065(2)	0.2031(2)	$\frac{1}{4}$	25(1)
Ru2	4*e*	0.362(2)	0	0	0.0628(5)	66(6)
C1	6*h*	1	0.3244(8)	0.0687(8)	$\frac{1}{4}$	75(5)
C2	6*h*	1	0.0176(9)	0.2091(9)	$\frac{1}{4}$	70(2)
C3	6*h*	1	0.6115(9)	0.1213(9)	$\frac{1}{4}$	78(8)
C4	4*f*	0.47(3)	$\frac{1}{3}$	$\frac{2}{3}$	0.0036(9)	69(6)
$Tb_3Ru_{1.776(4)}C_{4.95(1)}$						
Tb1a	6*h*	0.743(2)	0.2694(1)	0.2689(1)	$\frac{1}{4}$	60(3)
Tb1b	6*h*	0.257(2)	0.2245(3)	0.2225(3)	$\frac{1}{4}$	79(8)
Tb2	6*h*	1	0.1417(1)	0.5094(1)	$\frac{1}{4}$	75(2)
Ru1	6*h*	1	0.5112(1)	0.1956(1)	$\frac{1}{4}$	68(3)
Ru2	4*e*	0.276(4)	0	0	0.0634(8)	14(8)
C1	6*h*	1	0.330(2)	0.070(2)	$\frac{1}{4}$	78(3)
C2	6*h*	1	0.018(2)	0.217(2)	$\frac{1}{4}$	72(6)
C3	6*h*	1	0.602(3)	0.115(3)	$\frac{1}{4}$	77(9)
C4	4*f*	0.45(1)	$\frac{1}{3}$	$\frac{2}{3}$	0.009(9)	70(8)

[a]Two sets of data obtained from two crystals (I and II) of two different samples of $Gd_3Ru_2C_5$ were refined. The atomic positions were standardized by the program STRUCTURE TIDY (22). The rightmost column contains the isotropic displacement parameters U (pm^2) of the carbon and the equivalent isotropic U values of the anisotropic displacement parameters of the metal atoms.

TABLE 5
Interatomic Distances in the Structures of $R_3Ru_2C_5$ (R = Gd, Tb)[a]

		$Gd_3Ru_2C_5$ (I)	$Tb_3Ru_2C_5$			$Gd_3Ru_2C_5$ (I)	$Tb_3Ru_2C_5$
*R*1a:	1C3	242.1(9)	242(2)	Ru1:	1C1	187.7(7)	182(2)
	1C2	255.0(8)	250(3)		1C3	189.4(9)	189(1)
	1C1	262.5(8)	261(2)		1C3	209(1)	204(2)
	2C2	262.8(2)	258.6(6)		2C4	211(3)	209(3)
	2C1	263.2(2)	259.9(6)		2Ru1	296.2(1)	288.6(2)
	1C2	284.3(8)	296(3)		1*R*1a	319.4(1)	319.4(2)
	2Ru2	314.5(2)	314.1(2)		2*R*2	319.7(1)	313.3(1)
	1Ru1	319.4(1)	319.4(2)		2*R*2	325.6(1)	315.4(1)
	2Ru2	339.6(2)	341.5(2)		1*R*2	327.1(1)	331.1(2)
	2*R*2	351.2(1)	341.4(1)		1*R*1b	331.9(2)	336.6(3)
	1*R*2	357.3(1)	362.7(2)		2*R*1a	362.1(1)	356.6(1)
	2Ru1	362.1(1)	356.6(1)		2*R*1b	386.3(2)	385.2(3)
	2*R*1b	374.0(2)	370.4(3)	Ru2:	3C2	[249.1(5)	247(2)]
	2*R*1b	376.5(2)	375.6(2)		2Ru2	252.4(1)	247.3(1)
	1*R*2	388.4(1)	379.2(5)		3*R*1b	276.1(3)	274.3(4)
	4*R*1a	390.7(1)	390.1(1)		3C2	[278.6(5)	281(1)]
*R*1b:	1C2	227.6(8)	222(3)		3*R*1b	301.7(3)	296.3(4)
	1C1	251.3(7)	248(2)		3*R*1a	314.5(2)	314.1(2)
	1C2	252.3(9)	253(3)		1Ru2	316.0(5)	319.9(8)
	2C2	253.9(1)	248.9(3)		3*R*1a	339.6(2)	341.5(2)
	2C1	273.3(3)	272.1(7)	C1:	1C2	132.6(9)	142(3)
	2Ru2	276.1(3)	274.3(4)		1Ru1	187.7(7)	182(2)
	1C3	283.2(9)	284(2)		1*R*1b	251.3(7)	248(2)
	2Ru2	301.7(3)	296.3(4)		1*R*2	260.5(7)	263(2)
	1Ru1	331.9(2)	336.6(3)		1*R*1a	262.5(8)	261(2)
	4*R*1b	356.1(2)	351.2(3)		2*R*1a	263.2(2)	259.9(6)
	2*R*1a	374.0(2)	370.4(3)		2*R*1b	273.3(3)	272.1(7)
	2*R*1a	376.5(2)	375.6(2)	C2:	1C1	132.6(9)	142(3)
	2*R*2	380.9(2)	372.7(3)		1*R*1b	227.6(8)	222(3)
	2Ru1	386.3(2)	385.2(3)		2Ru2	[249.1(5)	247(2)]
	1*R*2	[402.5(3)	402.3(4)]		1*R*1b	252.3(9)	253(3)
*R*2:	2C4	246(1)	244(3)		2*R*1b	253.9(1)	248.9(3)
	2C3	252.4(1)	252(2)		1*R*1a	255.0(8)	250(3)
	1C1	260.5(7)	263(2)		2*R*1a	262.8(2)	258.6(6)
	1C3	278(1)	276(2)		2Ru2	[278.6(5)	281(1)]
	1C2	299.3(6)	298(2)		1*R*1a	284.3(8)	296(3)
	2Ru1	319.7(1)	313.3(1)		1*R*2	299.3(6)	298(2)
	2Ru1	325.6(1)	315.4(1)	C3:	1Ru1	189.4(9)	189(1)
	1Ru1	327.1(1)	331.1(2)		1Ru1	209(1)	204(2)
	2*R*1a	351.2(1)	341.4(1)		1*R*1a	242.1(9)	242(2)
	1*R*1a	357.3(1)	362.7(2)		2*R*2	252.4(1)	252(2)
	2*R*2	367.8(1)	367.0(2)		1*R*2	278(1)	276(2)
	2*R*1b	380.9(2)	372.7(3)		1*R*1b	283.2(9)	284(2)
	2*R*2	383.5(1)	386.5(2)	C4:	3Ru1	211(3)	209(3)
	1*R*1a	388.4(1)	379.2(5)		3*R*2	246(1)	244(3)
	1*R*1b	[402.5(3)	402.3(4)]				

[a]All distances shorter than 440 pm (*R*–*R*, *R*–Ru), 320 pm (*R*–C, Ru–C), 200 pm (C–C) are listed. Neighbors with distances listed in brackets are not shown in Fig. 5. The *R*1a, *R*1b, Ru2, and the C4 positions have occupancies of approximately only $\frac{3}{4}$, $\frac{1}{4}$, $\frac{1}{3}$, and $\frac{1}{2}$, respectively. These occupancies have to be accounted for in counting the number of near neighbors. Thus, for instance, an average Gd1 atom (Gd1a and Gd1b) has only four thirds of a Ru2 neighbor. Similarly, a Ru1 atom has on average approximately only one C4 neighbor.

C3, 93(5). For the crystal II of $Gd_3Ru_2C_5$ these occupancy values varied between 94(3) for C3 and 103(3) for C1. For $Tb_3Ru_2C_5$ they varied between 92(6) for C3 and 100.9(3) for Tb2. Thus, within three standard deviations these positions were found to be fully occupied and we have used the ideal occupancy parameters for these positions in all final least-squares runs. The atomic parameters for the three structure refinements and the interatomic distances for one (the more accurate) data set of $Gd_3Ru_2C_5$ as well as the interatomic distances of $Tb_3Ru_2C_5$ are listed in the Tables 4 and 5.

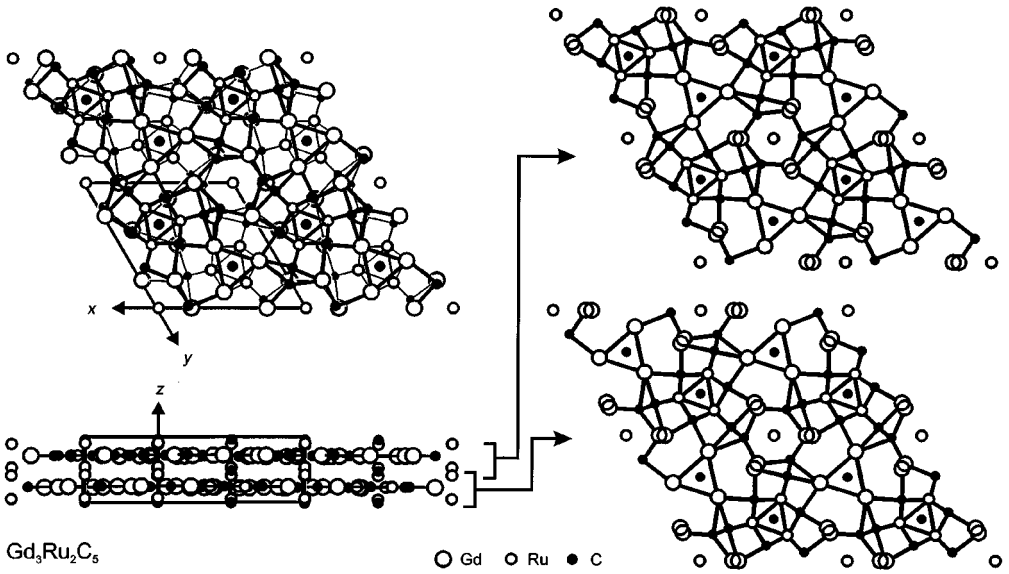

FIG. 4. Crystal structure of the hexagonal gadolinium ruthenium carbide $Gd_3Ru_2C_5$. Two equivalent atomic layers at $z = \frac{1}{4}$ and $\frac{3}{4}$ can be discerned. The lines connecting the atoms do not necessarily represent chemical bonds. Bonding within and between the layers is of approximately equal strength. The split positions Gd1a/Gd1b are shown only in the layers at the right-hand side of the figure.

DISCUSSION

The six ternary carbides $R_3Ru_2C_5$ (R = Y, Gd–Er) crystallize with a new structure type which we have refined for three data sets. The two data sets of the gadolinium compound were collected from two crystals isolated from two different samples both with the overall composition Gd:Ru:C = 35:20:45. It can be seen from the somewhat differing cell volumes (Fig. 1) that the compounds have noticeable homogeneity ranges. Since the two crystals of $Gd_3Ru_2C_5$ were taken from samples with the same overall composition, it is not surprising that the occupancy parameters of those atomic positions, which are not fully occupied, are similar. In contrast, the crystal of $Tb_3Ru_2C_5$ was isolated from a sample with considerable lower ruthenium content (Tb:Ru:C = 39:11:50). It has a lower occupancy for the Ru2 position (27.6% vs 35.1 and 36.2% for the two refinements of the gadolinium compound), and it also has a smaller cell volume than that observed for the terbium compound in the sample of the overall composition 35:20:45 (Fig. 1). Hence, the variation in the cell volumes can be ascribed to the variable occupancy of the Ru2 position. The cell volume of the yttrium compound fits in between those of the dysprosium and holmium compounds, as is frequently observed for carbides of the rare earth elements (23).

The structure was first determined for the crystal I of $Gd_3Ru_2C_5$. This is also the structure determination with the highest accuracy (i.e., the lowest standard deviations of the atomic parameters), in spite of its relatively high R values. For these reasons we will in the following discussion

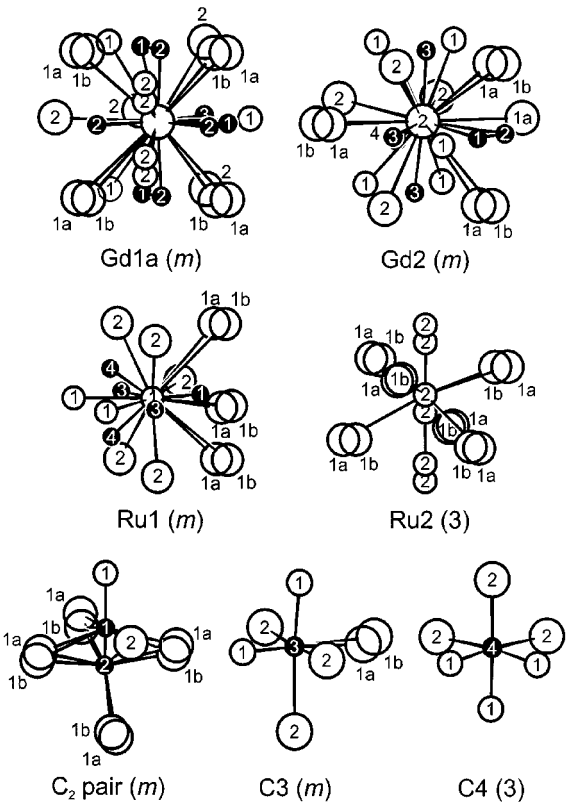

FIG. 5. Near-neighbor environments in the structure of $Gd_3Ru_2C_5$. The site symmetries are indicated in parentheses. For the split Gd1a/Gd1b position the coordination for both positions is shown. However, only the central atom Gd1a is drawn. The Gd1b position is located in front of the Gd1a position; it has the shorter distances to the Ru2 atoms.

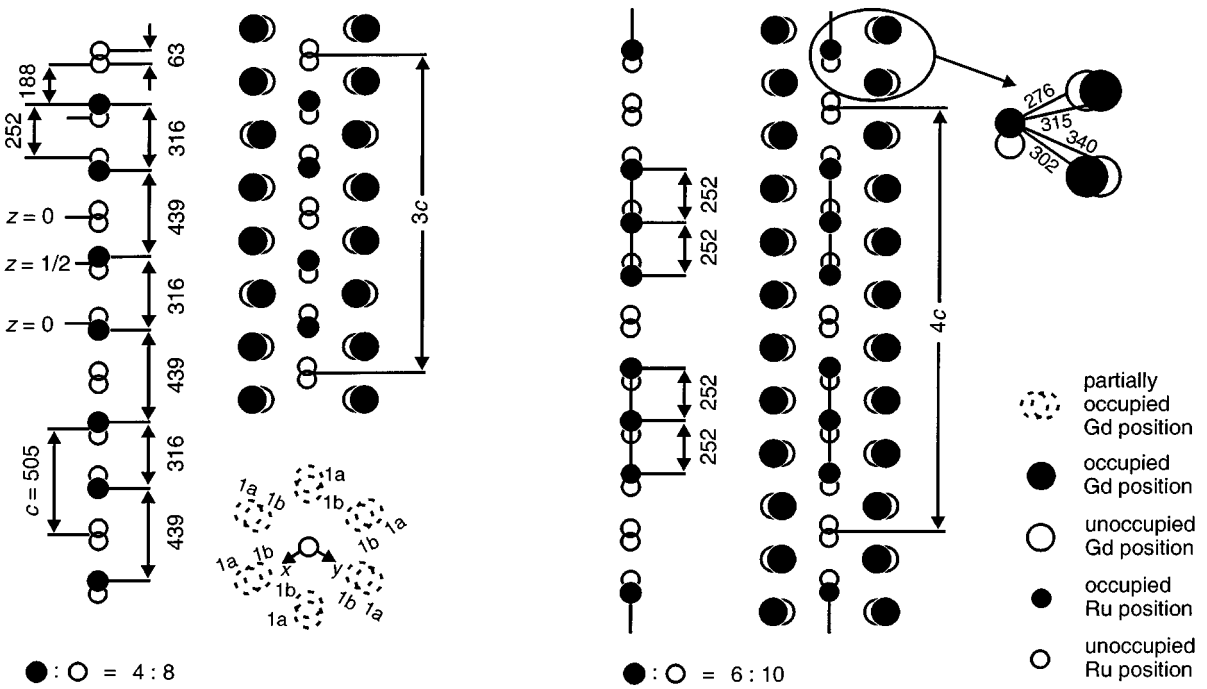

FIG. 6. Atomic environments of the Ru2 atoms. The Ru2 atoms are situated on the hexagonal axis 0, 0, z with split positions and a total observed occupancy of approximately $\frac{1}{3}$. Occupied positions are indicated by filled circles. The dotted circles on the left-hand side of the figure indicate the atomic positions of the Gd1a and Gd1b atoms as viewed in a projection along the hexagonal axis. Two different occupation patterns (idealized models for the atomic order) are shown. On the left-hand side, the ratio of occupied to unoccupied Ru positions is 4:8, on the right-hand side it is 6:10. The Gd1a and Gd1b occupancies are such that too-short Gd–Ru distances are avoided. The ratio of occupied Gd1a: Gd1b positions is 12:6 on the left-hand side; on the right-hand side it is 18: 6 per resulting translation period ($3c$ on the left-hand side and $4c$ on the right-hand side). The observed ratio of occupied Gd1a: Gd1b positions is approximately 75%:25%. The occupation pattern shown on the left-hand side avoids short Ru–Ru distances, that shown on the right-hand side leads to linear Ru_3 clusters. The latter occupation pattern is favored by the occupancies found for the Gd1a/Gd1b positions as well as by structure–chemical arguments.

describe the structure for this compound and quote distances as obtained for crystal I.

In the $Gd_3Ru_2C_5$ type structure most atoms are located on two equivalent mirror planes at $z = \frac{1}{4}$ and $\frac{3}{4}$ which are outlined in Fig. 4. The only exceptions are the atoms situated on the threefold axes: the C4 and Ru2 positions, both are located close to $z = 0$ and $\frac{1}{2}$, and both have partial occupancies. The structure contains several partially occupied atomic sites, all on or near the hexagonal 6_3 and $\bar{6}$ axes. This complicates the discussion of the near-neighbor coordinations. Nevertheless, it is possible to rationalize these environments.

The Gd1 atoms occupy a site close to the split positions of the Ru2 atoms, and for that reason the Gd1 atoms also occupy split positions, designated Gd1a and Gd1b, which are 49 pm apart. The Gd1a position has a much higher occupancy (75.3%) than the Gd1b position. The occupancy of both sites together was found to be very close to 100% during the structure refinements, and it was constrained to this ideal value in the final refinement cycles. In Fig. 5 we show the near-neighbor environments of this Gd1a/Gd1b position. It has 8 carbon neighbors in an irregular arrangement. Six of these carbon neighbors are (C1–C2) pairs of which both carbon atoms are direct neighbors of the central Gd1 atom, i.e., a side-on coordination. The Gd–C distances cover the range from 242 to 284 pm for Gd1a; for Gd1b this range extends from 228 to 283 pm. Each Gd1 atom (Gd1a as well as Gd1b) also has three Ru1 neighbors at distances between 319.4 and 386.3 pm. Of these, certainly the shorter ones should be considered as bonding distances in view of the fact that the sum of the metallic radii (for coordination number CN = 12) of gadolinium ($r = 180.1$ pm) and ruthenium ($r = 133.9$ pm), as calculated by us from the data compiled by Donohue (24) amounts to 314 pm. In addition, Table 5 lists for each Gd1 atom four Ru2 neighbors at distances between 276.1 and 363.1 pm. Since only one-third of the Ru2 positions are occupied, each Gd1 atom obtains on average only $\frac{4}{3}$ Ru2 neighbors, and the short Gd1b–Ru2 interactions of 276.1 pm do not need to occur. Furthermore, the Gd1 atoms have gadolinium neighbors at distances almost continuously covering the range from 351.2 to 402.5 pm. These also should be counted as bonding interactions,

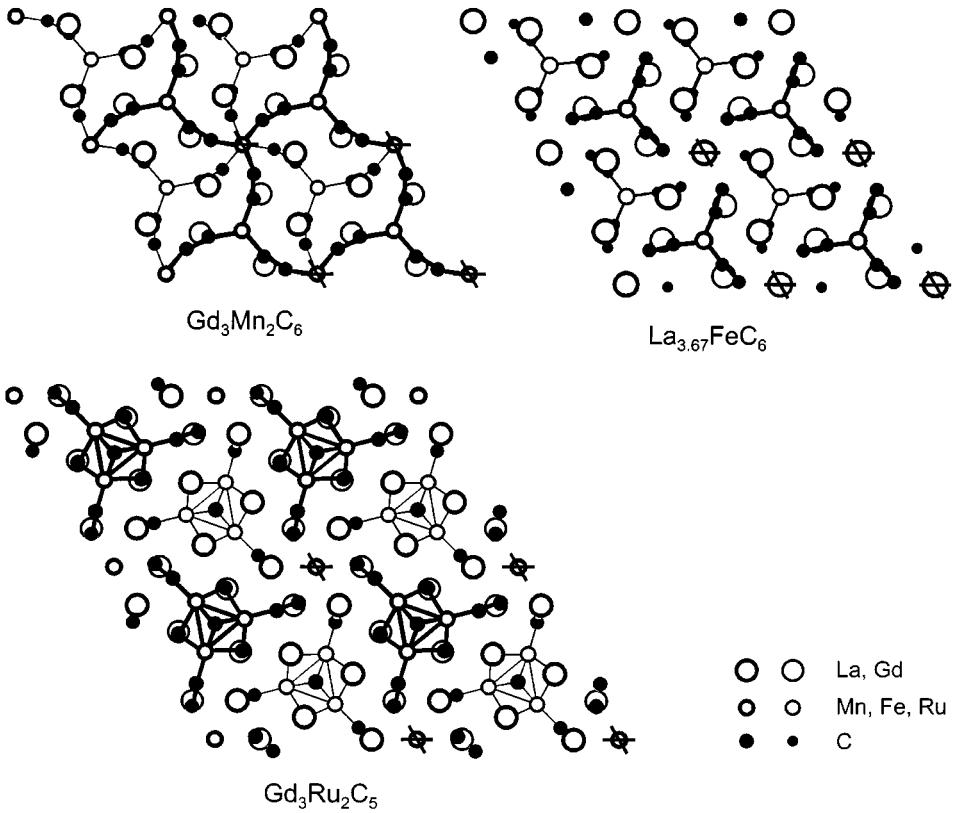

FIG. 7. The structure of $Gd_3Ru_2C_5$ as compared to the structures of $Gd_3Mn_2C_6$ and $La_{3.67}FeC_6$. Most atoms of these hexagonal structures (all with the same space group $P6_3/m$) are situated at $z = \frac{1}{4}$ (thin) and $\frac{3}{4}$ (thick lines). The origins of the unit cells are marked by crosses. The transition metal carbon polyanions of the three structures are outlined.

considering that the Gd–Gd distances in the hexagonal close-packed structure of elemental gadolinium amount to 357.1 and 363.3 pm.

The Gd2 atoms have six carbon neighbors; of the two C4 neighbors listed in Table 5, only one has to be counted, since the occupancy of the C4 position is approximately $\frac{1}{2}$. These six carbon neighbors of the Gd2 atoms are at an average distance of 264.9 pm, slightly larger than the average distances of 262.0 and 258.6 pm of the Gd1a and Gd1b atoms to their eight carbon neighbors. If the Gd atoms were forming bonds only to carbon atoms, we would expect the average Gd–C distances to be larger for the atoms with the higher coordination numbers. Since this is not the case, we compare the other neighbors of the gadolinium atoms. Indeed, as pointed out above, the Gd1a and Gd1b atoms have on average only approximately four ruthenium neighbors. In contrast, the Gd2 atoms have five Ru neighbors at an average distance of only 323.5 pm. Thus, in counting both the carbon and the ruthenium neighbors, and considering the bond strengths, the Gd1 and Gd2 atoms have comparable coordinations. In addition, like the Gd1 atoms, the Gd2 atoms form Gd–Gd bonds at distances comparable to those of the Gd1 atoms.

The Ru1 atoms have four carbon neighbors (only approximately one of the two neighboring C4 positions is occupied) at distances between 187.7 and 211 pm. All of these carbon neighbors are strongly bonded in view of the sum of the metallic radius (CN 12) of a ruthenium atom and the single-bond radius of the carbon atom: 134 pm + 77 pm = 211 pm. In addition, the Ru1 atoms have two Ru1 neighbors at a bonding distance of 296 pm. Together with the C1, C3, and C4 atoms, the Ru1 atoms form a trigonal Ru_3C_{10} cluster, which we discuss below.

In contrast, the Ru2 atoms have no carbon neighbors. They occupy a split position on the hexagonal 6_3 axis which is surrounded only by the Gd1a and Gd1b atoms. In Fig. 6 we show two different occupation patterns for these positions aiming for the observed occupancies of the Gd1a ($\sim 75\%$), Gd1b ($\sim 25\%$), and the Ru2 positions ($\sim 35\%$) as well as avoiding impossibly short interatomic distances. The main difference between the two patterns can be seen in the Ru2–Ru2 distances. These alternate between 316 and 439 pm in the model shown on the left-hand side of Fig. 6. Thus, in this model there are no strongly bonding Ru2–Ru2 interactions. In the model shown on the right-hand side, the Ru2 atoms form linear Ru_3 clusters with

rather short Ru2–Ru2 distances of 252.4 pm. We favor the latter model, because it allows a higher electron count for the Ru2 atoms. The magic number of 18 electrons per Ru2 atom can be reached only if the Ru2–Ru2 interactions are formally counted as triple or quadruple bonds as is further discussed below. This model with a Gd1a/Gd1b site occupancy of 18:6 is also favored by the ratio of the observed site occupancies of 75:25%, in contrast to the other model with a theoretical Gd1a/Gd1b occupancy of 12:6.

Of the carbon atoms the C1 and C2 atoms form pairs with a C1–C2 distance of 132.6(9) pm, quite close to the typical double-bond distance of 134 pm in olefins. These pairs are situated in octahedra formed by four Gd1, one Gd2, and one Ru1 atom (Fig. 5). The C3 and C4 atoms have octahedral metal coordinations of 4 Gd + 2 Ru and 3 Gd + 3 Ru, respectively.

The structure of $Gd_3Ru_2C_5$ shows some similarity with the structures of $Gd_3Mn_2C_6$ (25) and $La_{3.67}FeC_6$ (6). The three structures are compared in Fig. 7, where their transition metal carbon polyanions are emphasized. They all crystallize in the same space group ($P6_3/m$), have similar metal-to-carbon ratios of 5:6, 4.67:6, and 5:5, and contain C_2 pairs. However, the structure of $Gd_3Ru_2C_5$ contains, in addition to the C_2 pairs, also isolated carbon atoms, and its cell content (Z) is twice as large as that of the others.

Frequently, chemical bonding in ternary rare earth transition metal carbides can be rationalized with simple concepts using the Lewis notation and aiming for electron counts of 18 and 8 for the transition metal and carbon atoms, respectively (7, 8, 10, 15, 23, 25, 26). This is to some extent also possible for $Gd_3Ru_2C_5$, although the partially occupied sites complicate this account. For simplicity, we assume somewhat idealized occupancies of $\frac{3}{4}$, $\frac{1}{4}$, $\frac{1}{3}$, and $\frac{1}{2}$ for the sites of Gd1a, Gd1b, Ru2, and C4, respectively. These correspond to the composition $Gd_3Ru_{1.83}C_5$, which is very close to the compositions $Gd_3Ru_{1.851(1)}C_{4.86(2)}$ and $Gd_3Ru_{1.862(2)}C_{4.97(3)}$ resulting from the two structure refinements. In Fig. 8 we show the trigonal Ru_3C_{10} cluster which is surrounded only by gadolinium atoms. It is completely planar with the exception of the C4 atom which is situated above or below the Ru_3 triangle. In the lower part of Fig. 8 we show a valence electron distribution using the Lewis formalism, where each line represents two electrons; a dashed line represents one electron. It can be seen that the ruthenium and carbon atoms obtain electron counts of 18 and 8, respectively. That means that they utilize all available valance orbitals for chemical bonding. This cluster obtains a formal charge of −13. The electrons shown as lone pairs at the carbon atoms are forming bonds with the gadolinium atoms. If we count the electrons forming Ru–C bonds at the carbon atoms we can represent the Ru_3C_{10} cluster with the formula $\{(Ru1^{5+})_3[(C1\text{–}C2)^{4-}]_3(C3^{4-})_3C4^{4-}\}^{13-}$ where the superscripts are oxidation numbers.

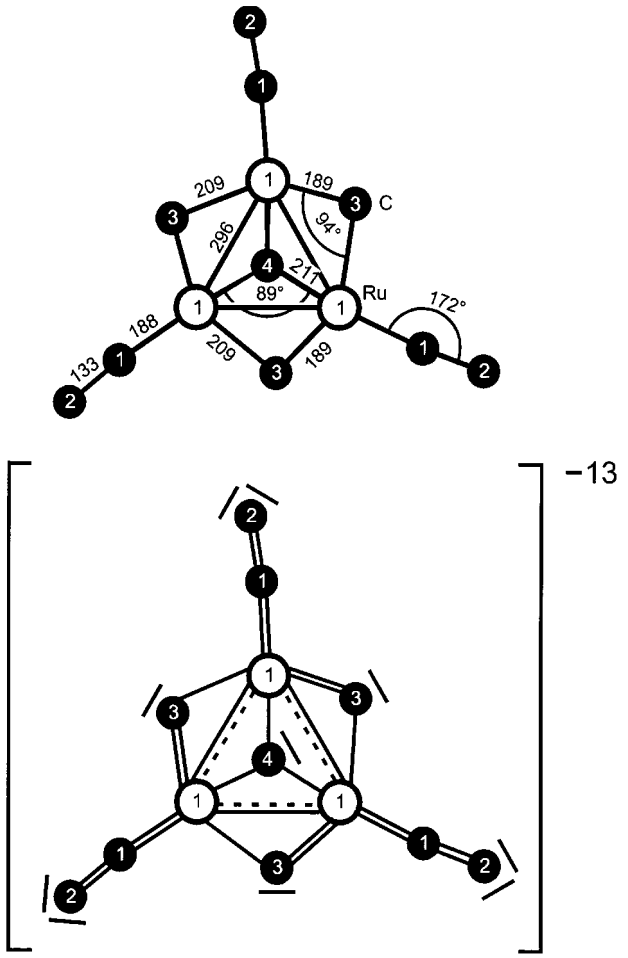

FIG. 8. The polyanionic Ru_3C_{10} cluster in the structure of $Gd_3Ru_2C_5$. All atoms of this trigonal cluster are coplanar with the exception of the C4 atom, which is located statistically at a distance of 126 pm above or below that plane. Single-digit numbers correspond to the atom designations. Interatomic distances (pm) are given in the upper part of the drawing. In the lower part a possible valence electron distribution is shown, using the Lewis formalism where each continuous line represents two electrons; dashed lines represent one electron. Electrons shown as lone pairs at the carbon atoms form bonds with the gadolinium atoms. With this valence electron distribution the carbon and ruthenium atoms have electron counts of 8 and 18, respectively. The resulting formal charge of this complex is −13.

The Ru2 atoms have no carbon neighbors. They are distributed on a fourfold site with an occupancy of approximately $\frac{1}{3}$. They can reach electron counts of 18 only by forming linear Ru_3 clusters as shown on the right-hand side of Fig. 9, where these clusters obtain formal charges of −18 and −14, respectively. The resulting formulas for the whole compound are $[Gd_{54}]^{153+}\{[(Ru2_3)^{18-}]_2\}^{36-}\{[(Ru1_3C_{10})^{13-}]_9\}^{117-}$, and $[Gd_{54}]^{+145}\{[(Ru2_3)^{14-}]_2\}^{28-}\{[(Ru1_3C_{10})^{13-}]_9\}^{117-}$, respectively, or $(Gd_3)^{8.5+}(Ru2_{0.33})^{2-}[(Ru1_3C_{10})_{0.5}]^{6.5-}$, and $(Gd_3)^{+8.06}(Ru2_{0.33})^{1.56-}[(Ru1_3C_{10})_{0.5}]^{6.5-}$. Thus, on average, each gadolinium

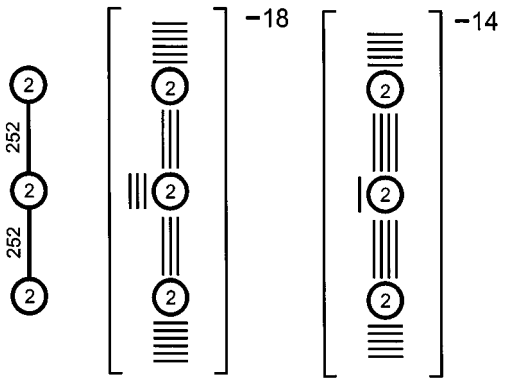

FIG. 9. Possible valence electron distributions in the linear Ru_3 cluster of the Ru2 atoms in $Gd_3Ru_2C_5$. This cluster is surrounded only by gadolinium atoms. The electrons forming Gd–Ru2 bonds are all counted at the Ru2 atoms. Thus, the cluster obtains large negative formal charges of −18 or −14, respectively, as shown on the right-hand side. In both valence electron distributions the Ru2 atoms obtain electron counts of 18. The valence electron distribution with the formal charge of −14 is favored, because it allows for Gd–Gd bonding, as is discussed in the text.

atom retains only 0.17 or 0.31 electrons, respectively, for Gd–Gd bonding. We have discussed above that the Gd–Gd bonding cannot be neglected. For this reason we prefer the electron count of − 14 for the $Ru2_3$ cluster. Certainly, this electron counting can only be a crude approximation; however, it allows to rationalize the observed interatomic distances, and it may serve as a take-off point for more elaborate bonding models.

ACKNOWLEDGMENTS

We thank Dipl.-Ing. U. Ch. Rodewald and Dr. M. H. Möller for the competent collection of the single-crystal diffractometer data, Dr. B. Künnen for the electrical conductivity measurements, as well as Mr. H.-J. Göcke and Mr. K. Wagner for the work at the scanning electron microscope. We also acknowledge Dr. W. Gerhartz (Degussa AG) and Dr. G. Höfer (Heraeus Quarzschmelze) for generous gifts of the ruthenium powder and silica tubes, respectively. This work was also supported by the Deutsche Forschungsgemeinschaft, the Fond der Chemischen Industrie, and the International Centre for Diffraction Data.

REFERENCES

1. H. Holleck, *J. Less-Common Met.* **52,** 167 (1977).
2. H. Holleck, *J. Nucl. Mater.* **42,** 278 (1972).
3. D. G. Parnell, N. H. Brett, and P. E. Potter, *J. Less-Common Met.* **114,** 161 (1985).
4. K. H. Wachtmann, M. A. Moss, R.-D. Hoffmann, and W. Jeitschko, *J. Alloys Compd.* **219,** 279 (1995).
5. R.-D. Hoffmann, R. Pöttgen, and W. Jeitschko, *J. Solid State Chem.* **99,** 134 (1992).
6. A. M. Witte and W. Jeitschko, *Z. Naturforsch.* **51b,** 249 (1996).
7. M. W. Pohlkamp, G. Kotzyba, U. A. Böcker, M. H. Gerdes, K. H. Wachtmann, and W. Jeitschko, *Z. Anorg. Allg. Chem.* **627,** 341 (2001).
8. R.-D. Hoffmann, K. H. Wachtmann, Th. Ebel, and W. Jeitschko, *J. Solid State Chem.* **118,** 158 (1995).
9. U. E. Musanke, W. Jeitschko, and R.-D. Hoffmann, *Z. Kristallogr.* **205,** 201 (1993).
10. R.-D. Hoffmann and W. Jeitschko, *Acta Crystallogr. B* **54,** 834 (1998).
11. R.-D. Hoffmann and W. Jeitschko, *Acta Crystallogr. A* **46,** C-285 (1990).
12. K. Yvon, W. Jeitschko, and E. Parthé, *J. Appl. Crystallogr.* **10,** 73 (1977).
13. R. Welter, G. Venturini, and B. Malaman, *J. Alloys Compd.* **189,** 49 (1992).
14. M. E. Danebrock, W. Jeitschko, A. M. Witte, and R. Pöttgen, *J. Phys. Chem. Solids* **56,** 807 (1995).
15. M. H. Gerdes, W. Jeitschko, K. H. Wachtmann, and M. E. Danebrock, *J. Mater. Chem.* **7,** 2427 (1997).
16. M. W. Wolff, S. Niemann, Th. Ebel, and W. Jeitschko, *J. Magn. Magn. Mater.* **223,** 1 (2001).
17. M. H. Gerdes, A. M. Witte, W. Jeitschko, A. Lang, and B. Künnen, *J. Solid State Chem.* **138,** 201 (1998).
18. W. Jeitschko, Th. Konrad, K. Hartjes, A. Lang, and R.-D. Hoffmann, *J. Solid State Chem.* **154,** 246 (2000).
19. W. Jeitschko, A. J. Foecker, D. Paschke, M. V. Dewalsky, Ch. B. H. Evers, B. Künnen, A. Lang, G. Kotzyba, U. Ch. Rodewald, and M. H. Möller, *Z. Anorg. Allg. Chem.* **626,** 1112 (2000).
20. B. Künnen, D. Niepmann, and W. Jeitschko, *J. Alloys Compd.* **309,** 1 (2000).
21. G. M. Sheldrick, "SHELX-97, A Program System for the Solution and Refinement of Crystal Structures." Universität Göttingen, Germany, 1997.
22. L. M. Gelato and E. Parthé, *J. Appl. Crystallogr.* **20,** 139 (1987).
23. W. Jeitschko, G. Block, G. E. Kahnert, and R. K. Behrens, *J. Solid State Chem.* **89,** 191 (1990).
24. J. Donohue, "The Structures of the Elements." Wiley, New York, 1974.
25. G. E. Kahnert and W. Jeitschko, *Z. Anorg. Allg. Chem.* **619,** 93 (1993).
26. R. B. King, *J. Organomet. Chem.* **536/537,** 7 (1997).